



Spectral-based estimation of components concentration in skin tissue layers with independence of shading via optical modeling of skin tissue

Kaito Iuchi¹ · Takanori Igarashi² · Nobutoshi Ojima³ · Keiko Ogawa-Ochiai⁴ · Norimichi Tsumura⁵

Received: 14 July 2021 / Accepted: 7 December 2021
© International Society of Artificial Life and Robotics (ISAROB) 2022

Abstract

Analysis of concentration of components in skin tissue, such as melanin, blood, oxygen saturation, is important in medical or cosmetic fields. Some researchers have developed methods to estimate the components. However, almost all the research has not considered a depth dependency of blood concentration and oxygen saturation, which is actual characteristic of skin tissue. Although there has been a method considering the depth dependency, the method does not have capability to estimate oxygen saturation. In addition, there is a problem in the methods that it is possible that the estimation is disturbed by shading which is on skin surface. Therefore, in this paper, we propose a method solving those problems of the methods, that is to estimate melanin concentration, blood concentration, and oxygen saturation in skin tissue layers with independence of shading considering the depth dependency. The proposed method is evaluated on the estimation accuracy with simulation comparing previous methods. The result indicates preferred capability of the proposed method.

Keywords Skin tissue · Melanin · Blood · Hemoglobin · Oxygen saturation · Monte Carlo simulation · Spectral reflectance

1 Introduction

Skin is one of the most important factors in human from a standpoint of medical or cosmetic. Skin is the largest organ in human body, which covers an entire surface of a human body with a thickness of several millimeters. Skin has a part of roll to interact with ambient environment such as thermoregulation and cutaneous sensation. In addition, skin chiefly determines apparent impression of age, health, or beauty. In spite of the importance, skin much more likely

to suffer from an injury or a disorder due to the exposure to ambient environment. Thus, there is a need of an objective and quantitative method to diagnose skin. The solution to the needs would be monitoring skin components which are melanin concentration, blood concentration, and oxygen saturation. It is because that skin disorders cause abnormality of those skin components, since skin disorders occur mainly in an epidermis layer or dermis layer of skin tissue where there are those skin components [1].

There are various methods to estimate those skin components [2–6]. In terms of required information to estimate those skin components those methods are divided into two methods, which are RGB-based method or spectral-based method. Spectral-based method is indicated to have capability of more accurate estimation than RGB-based method due to difference of the amount of information [3–7]. The spectral-based method proposed by Akaho et al. have most accuracy of estimation [7]. However, in Akaho's method, there could be influence of shading as noise since the method estimate shading due to a shape of the measurement location and lighting unevenness along with skin components. Thus, it is desirable to solve the limitation on shading.

In addition, there is another important limitation in those RGB-based or spectral-based methods, which is on structure

✉ Kaito Iuchi
k.iuchi@chiba-u.jp

¹ Department of Imaging Science, Graduate School of Science and Engineering, Chiba University, Chiba, Japan

² Skin Care Products Research Lab, Kao Corporation, Tokyo, Japan

³ Personal Health Care Products Research Lab, Kao Corporation, Tokyo, Japan

⁴ Department of General Medicine, Kampo Clinical Center, Hiroshima University Hospital, Hiroshima, Japan

⁵ Department of Imaging Science, Graduate School of Engineering, Chiba University, Chiba, Japan

of assumed skin model. In those methods, it is assumed that there are simply two layers in skin tissue: epidermis or dermis which uniformly distribute melanin or blood, respectively. However, blood is distributed in multiple layers: papillary dermis, upper blood net dermis, reticular dermis, deep blood net dermis, or subcutaneous dermis, which have different blood fluctuation in each layer [8]. Here, Iuchi et al. have proposed a method based on Akaho's method to consider unevenness of blood concentration depending on depth in skin tissue. However, Iuchi's method do not have capability to estimate oxygen saturation, because skin model constructed in the research is set to constant oxygen saturation. In addition, as with Akaho's method, there could be influence of shading as noise, since the method estimate shading due to a shape of the measurement location and lighting unevenness along with skin components. Thus, it is desirable to solve the limitation on oxygen saturation and shading.

Therefore, in this research, we propose a method to estimate melanin concentration, blood concentration, and oxygen saturation in skin tissue considering depth dependency of blood concentration with independence of shading. In addition, the conventional method that assumes that the blood distribution is uniform regardless of depth has merit that it can be estimated with only small amount of wavelength information and small computational cost compared to a method that considers the difference in blood distribution depending on the depth. Therefore, it is preferable to handling of the blood layer according to its applications. Therefore, in this research, two models with different handling of blood layers are constructed. Furthermore, the proposed method is evaluated on the estimation accuracy with simulation comparing previous methods.

2 Method to estimate components concentration of skin tissue

In this Chapter, we describe the proposed method to estimate melanin concentration, blood concentration and oxygen saturation in skin tissue with considering depth dependency of blood concentration with independence of shading. The proposed methods is based on machine learning so that it is need to learn based on a dataset. To construct a dataset, we obtain various sets of components concentration in skin tissue and corresponding spectral reflectance based on Monte Carlo simulation of light transport in multi-layered tissue (MCML) proposed by Wang et al. [9]. Specifically, the proposed method consists of the following three phases. As first phase, for conducting MCML, it is necessary to construct an optical skin model. As a base of an optical skin model, a seven-layered skin model is constructed. next, we construct two types of optical skin models with different setting of blood layers in skin tissue based on the 7-layered

skin model. As second phase, a dataset is constructed with each of the two skin models based on MCML. This dataset is composed of sets of components concentrations as explanation variable and a corresponding spectral reflectance as a target variable. As third phase, we estimate melanin concentration, blood concentration and oxygen saturation in skin tissue with independence of shading based on the constructed dataset.

2.1 Construction of a seven-layered skin model

For conducting MCML, it is necessary to define an optical skin model. In this research, two types of optical skin models which have different setting of blood layers in skin tissue is constructed based on a seven-layered skin model. There are five parameters set for each layer: thickness d , refractive index n , anisotropic parameter $g(\lambda)$, scattering coefficient $\mu_s(\lambda)$, and absorption coefficient $\mu_a(\lambda)$. Here, λ represents a wavelength [nm]. In a skin layer structure model, an anisotropic parameter $g(\lambda)$ and a scattering coefficient $\mu_s(\lambda)$ are generally considered not to vary depending on layers [1, 7, 8]. Next, the values of each parameter are explained in detail. Table 1 shows the seven-layered model of skin and the containing components, thickness and refractive index of each layer [10, 11]. The absorption coefficient $\mu_a(\lambda)$ are subscripted to distinguish the values of each layer. The subscripts of str are for stratum corneum, liv for living epidermis, pap for papillary dermis, upp for upper blood net dermis, ret for reticular dermis, dee for deep blood net dermis, and sub for subcutaneous dermis. Figure 1 shows the anisotropic parameter $g(\lambda)$ [8, 12]. Figure 2 shows the scattering coefficient $\mu_s(\lambda)$ [13]. The absorption coefficients of each layer are given by Eqs. (1), (2), (3), (4), (5), (6), and (7), respectively. [8, 10, 11, 14]:

$$\mu_{a,\text{str}}(\lambda) = \mu_{a,\text{base}}(\lambda), \quad (1)$$

$$\mu_{a,\text{liv}}(\lambda) = [\text{Mel}] \times \mu_{a,\text{Mel}}(\lambda) + (1 - [\text{Mel}]) \times \mu_{a,\text{base}}(\lambda), \quad (2)$$

$$\begin{aligned} \mu_{a,\text{pap}}(\lambda) = & \left\{ [\text{StO}]_{\text{pap}} \times [\text{Oxy-Hb}]_{\text{pap}} \times \mu_{a,\text{Oxy-Hb}}(\lambda) + (1 - [\text{StO}]_{\text{pap}}) \right. \\ & \left. \times [\text{DeOxy-Hb}]_{\text{pap}} \times \mu_{a,\text{DeOxy-Hb}}(\lambda) \right\} \\ & + \left\{ 1 - \left([\text{Oxy-Hb}]_{\text{pap}} + [\text{DeOxy-Hb}]_{\text{pap}} \right) \right\} \times \mu_{a,\text{base}}(\lambda), \end{aligned} \quad (3)$$

$$\begin{aligned} \mu_{a,\text{upp}}(\lambda) = & \left\{ [\text{StO}]_{\text{upp}} \times [\text{Oxy-Hb}]_{\text{upp}} \times \mu_{a,\text{Oxy-Hb}}(\lambda) + (1 - [\text{StO}]_{\text{upp}}) \right. \\ & \left. \times [\text{DeOxy-Hb}]_{\text{upp}} \times \mu_{a,\text{DeOxy-Hb}}(\lambda) \right\} \\ & + \left\{ 1 - \left([\text{Oxy-Hb}]_{\text{upp}} + [\text{DeOxy-Hb}]_{\text{upp}} \right) \right\} \times \mu_{a,\text{base}}(\lambda), \end{aligned} \quad (4)$$

Table 1 Contained components, thickness, and refractive index of each layer in a seven-layered skin model

Name of layer	Chromophore	Thickness [μm]	Refractive index
Stratum corneum	None	20	1.5
Living epidermis	Melanin	90	1.34
Papillary dermis	Oxy-hemoglobin	175	1.4
	Deoxy-hemoglobin		
Upper blood net dermis	Oxy-hemoglobin	90	1.39
	Deoxy-hemoglobin		
Reticular dermis	Oxy-hemoglobin	1500	1.4
	Deoxy-hemoglobin		
Deep blood net dermis	Oxy-hemoglobin	100	1.38
	Deoxy-hemoglobin		
Subcutaneous dermis	Oxy-hemoglobin	6250	1.44
	Deoxy-hemoglobin		

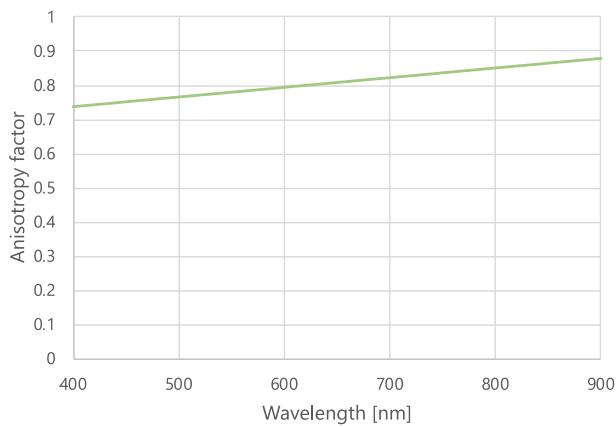


Fig. 1 Anisotropy factor

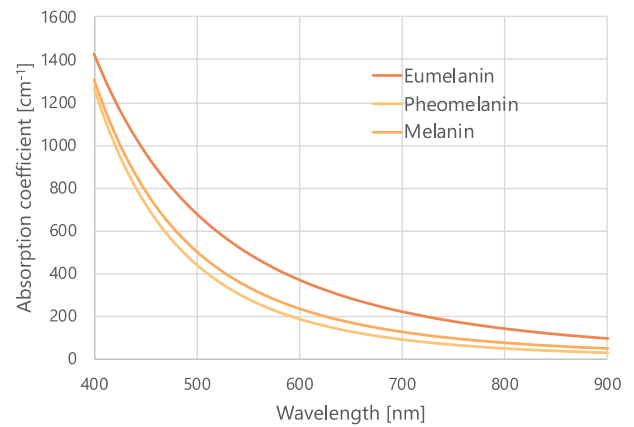


Fig. 3 Absorption coefficient of melanin

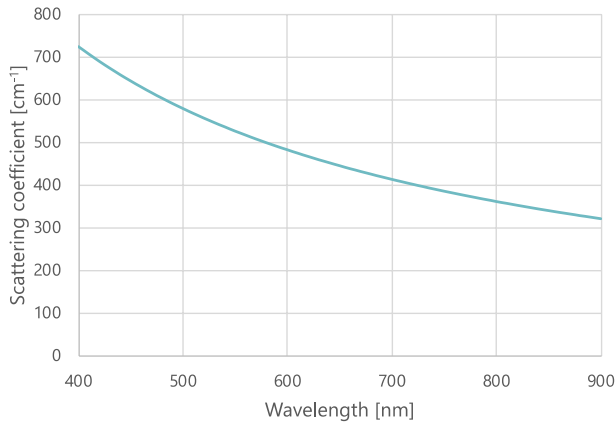


Fig. 2 Scattering coefficient

$$\begin{aligned} \mu_{a,ret}(\lambda) = & \{ [StO]_{ret} \times [Oxy-Hb]_{ret} \times \mu_{a,Oxy-Hb}(\lambda) + (1 - [StO]_{ret}) \\ & \times [DeOxy-Hb]_{ret} \times \mu_{a,DeOxy-Hb}(\lambda) \} \\ & + \{ 1 - ([Oxy-Hb]_{ret} + [DeOxy-Hb]_{ret}) \} \times \mu_{a,bas}(\lambda), \quad (5) \end{aligned}$$

$$\begin{aligned} \mu_{a,dee}(\lambda) = & \{ [StO]_{dee} \times [Oxy-Hb]_{dee} \times \mu_{a,Oxy-Hb}(\lambda) + (1 - [StO]_{dee}) \\ & \times [DeOxy-Hb]_{dee} \times \mu_{a,DeOxy-Hb}(\lambda) \} \\ & + \{ 1 - ([Oxy-Hb]_{dee} + [DeOxy-Hb]_{dee}) \} \times \mu_{a,base}(\lambda), \end{aligned} \tag{6}$$

$$\begin{aligned} \mu_{a,sub}(\lambda) = & \{ [StO]_{sub} \times [Oxy-Hb]_{sub} \times \mu_{a,Oxy-Hb}(\lambda) + (1 - [StO]_{sub}) \\ & \times [DeOxy-Hb]_{sub} \times \mu_{a,DeOxy-Hb}(\lambda) \} \\ & + \{ 1 - ([Oxy-Hb]_{sub} + [DeOxy-Hb]_{sub}) \} \times \mu_{a,base}(\lambda). \end{aligned} \tag{7}$$

Here, assuming that the entire volume of each layer is 100 [%], [Mel] is melanin concentration, [StO] is oxygen saturation, [Oxy-Hb] is oxy-hemoglobin concentration, and [DeOxy-Hb] is deoxy-hemoglobin concentration. The subscripts of each component concentration are str for stratum corneum, liv for living epidermis, pap for papillary dermis, upp for upper blood net dermis, ret for reticular dermis, dee for deep blood net dermis, and sub for subcutaneous dermis. The subscripts of the absorption coefficient μ_a are mel for melanin, Oxy-Hb for oxy-hemoglobin, DeOxy-Hb for deoxy-hemoglobin, and base for baseline, respectively. Here, the baseline is an absorption coefficient of the skin tissue in the area where there are no components [11, 14]. Figure 3 shows the absorption coefficient of melanin $\mu_{a,mel}(\lambda)$, the absorption coefficient of eumelanin, and the absorption coefficient of pheomelanin [11, 14]. Figure 4 shows the absorption coefficient $\mu_{a,base}(\lambda)$ of baseline [15]. The absorption coefficient $\mu_{a,Oxy-Hb}$ of oxy-hemoglobin and the absorption coefficient $\mu_{a,DeOxy-Hb}$ of deoxy-hemoglobin are shown in Fig. 5 [7, 8]. Oxygen saturation is defined by Eq. (8):

$$\text{Oxygen saturation} = \frac{[Oxy-Hb]}{[Oxy-Hb] + [DeOxy-Hb]}. \tag{8}$$

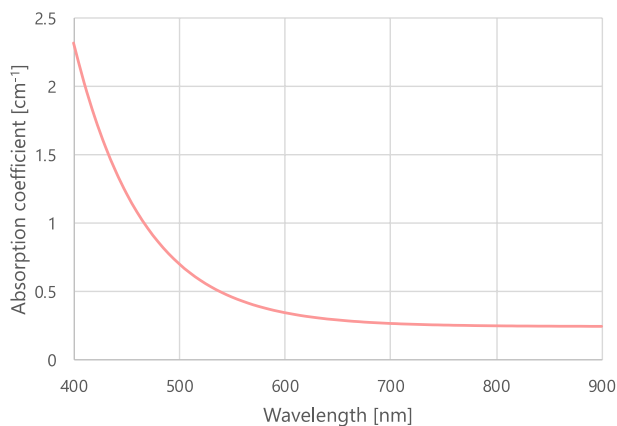


Fig. 4 Absorption coefficient of baseline

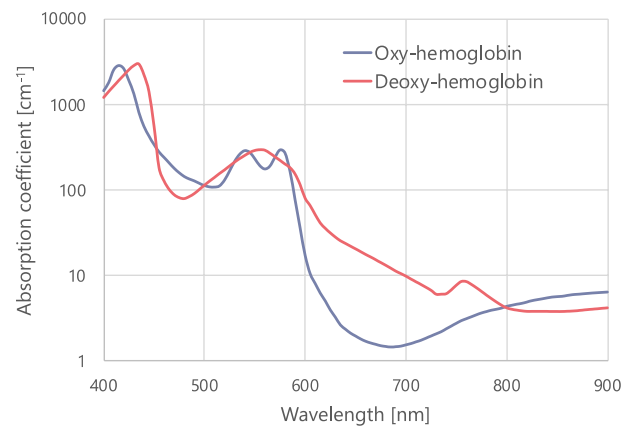


Fig. 5 Absorption coefficient of hemoglobin

2.2 Construction of two skin models based on the seven-layered skin model

As mentioned above, in this research, to make it possible to manage skin models with different setting of blood layers depending on applications, two skin models are constructed. Furthermore, the proposed method is established based on each of the models. Here, the skin models to be constructed is based on the seven-layered skin model described in the previous section.

Along with the previous method [3, 5–7, 14, 15], the four-layered skin model approximates distribution of blood in skin tissue to be uniform regardless of the depth. Thus, papillary dermis, upper blood net dermis, and reticular dermis in the seven-layered skin model constructed in Sect. 2.1 are comprehensively considered as a layer of dermis. Therefore, the four-layered model to be constructed is consisted of the stratum corneum layer containing no components, the epidermis layer containing melanin, the dermis layer containing blood, and the subcutaneous dermis layer.

The five-layered skin model is a model in which a blood layer excluding subcutaneous tissue in skin tissue is divided into a papillary layer and a reticular layer as with several studies which analyze the blood layer divided into two parts [8, 16, 17]. Thus, papillary dermis and upper blood net dermis in the seven-layered skin model constructed in Sect. 2.1

Table 2 Combinations of components set in four-layered skin model to construct dataset of four-layered skin model

Name of layer	Component	Range [%]	Sampling interval [%]	Total number
Epidermis	Melanin	1.0–10.0	0.50	19
Dermis	Blood	0.10–1.0	0.050	19
	Oxygen saturation	40–100	10.0	7

Table 3 Combinations of components set in five-layered skin model to construct dataset of five-layered skin model

Name of layer	Chromophore	Range [%]	Sampling interval [%]	Total number
Epidermis	Melanin	1.0–10.0	1.0	10
Papillary dermis	Blood	0.10–1.0	0.10	10
	Oxygen saturation	40–100	15.0	5
Reticular dermis	Blood	0.10–1.0	0.10	10
	Oxygen saturation	40–100	15.0	5

are comprehensively considered as a papillary layer, and reticular dermis layer and deep blood net dermis in the seven-layered skin model are comprehensively considered as a reticular layer. Therefore, the five-layered model to be constructed is consisted of stratum corneum containing no components, epidermis layer containing melanin, the papillary layer, reticular layer, and subcutaneous tissue containing blood.

In both models, the parameters such as the thickness d of each layer, refractive index n , anisotropic parameter $g(\lambda)$, scattering coefficient $\mu_s(\lambda)$, absorption coefficient $\mu_{a,pigment}$ of each component, absorption coefficient $\mu_{a,layer}$ of each layer are based on the 7-layered skin model described in Sect. 2.1.

2.3 Construction of dataset with the two sin models based on MCML

In this section, datasets are constructed based on the four-layered skin model or five-layered skin model. First, we conduct MCML to obtain spectral reflectances corresponding combinations of components concentration in skin tissue. The combinations of components concentration are shown in Tables 2 or 3 for the four-layered skin model or five-layered skin model, respectively. The total number of combinations is 2527 or 25,000 for the four-layered skin model or the five-layered skin

model, respectively. The spectral reflectances are obtained at 31 wavelengths which is sampled at 10 [nm] intervals between the visible light range from 400 to 700 [nm]. Figure 6 shows the obtained spectral reflectance data.

2.4 The method to remove influence of shading

This section describes a processing method which is performed onto the constructed datasets so as to remove influence of shading on the estimation of skin components concentration. Assuming the absorber and scatterer in skin tissue are oxy-hemoglobin, deoxy-hemoglobin, and melanin and an absorption by those absorbers is $Z(\lambda)$, an absorbance $Abs(\lambda)$ of any skin can be described in Eq. (9) based on Modified Lambert–Beer's law [2, 7, 8]:

$$Abs(\lambda) = Z(\lambda) + k. \tag{9}$$

Here, k is a shading component due to a shape of the measurement location and lighting unevenness. Assuming the spectral sensitivity of the sensor, the spectral transmittance of the sensor, and the spectral distribution of the light source are normalized, the shading component k is independent of wavelength. Taking this fact into consideration, as shown in Eq. (10), by normalizing an absorbance $Abs(\lambda)$ of any skin into a relative value $ReAbs(\lambda)$ from a certain

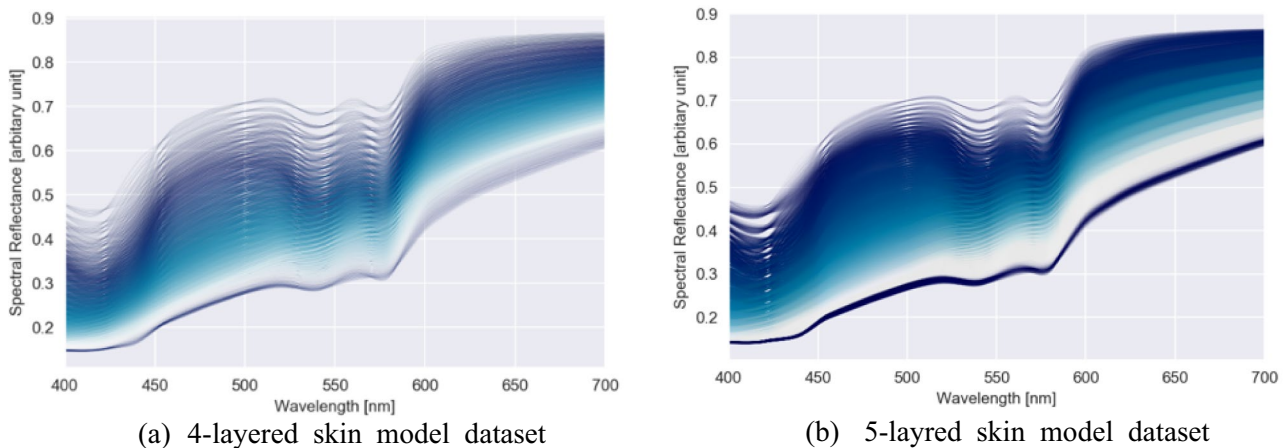


Fig. 6 Spectral reflectances acquired based on MCML

reference value, information of shading component k can be excluded from an absorbance $Abs(\lambda)$ of any skin:

$$ReAbs(\lambda) = Abs(\lambda) - Fnc(Abs(\lambda)). \tag{10}$$

Here, $Fnc()$ a function (hash function) which takes arbitrary data as input and takes a value (hash value) encapsulating the data as output by a specific algorithm. In Eq. (10), inputting an absorbance $Abs(\lambda)$ of an arbitrary skin to the hash function $Fnc()$, the absorbance $Abs(\lambda)$ is converted to the relative value $ReAbs(\lambda)$. Here, as an instance of an algorithm of the hash function $Fnc()$, a method is conceivable to extract an absorbance of a specific wavelength from an input absorbance data. However, if the hash function $Fnc()$ is dependent on a specific one wavelength, the hash function could have weak capability of noise robustness, because noise of absorbance of the wavelength is diffused throughout a relative absorbance due to the conversion due to the conversion of normalization based on the hash function and Eq. (10). Therefore, in this study, as the algorithm of the hash function $Fnc()$, we adopt a method to calculate an average value of an absorbance of all wavelengths within an input absorbance data. In this method, even if noise is on one specific wavelength, the influence of the noise is reduced by calculating the average value of the absorbances of all wavelengths. Thus, there is improvement of robustness against noise in averaging method. This is formulated as Eq. (11). N is a constant indicating the number of wavelengths. An absorbance of any skin converted by the algorithm shown in Eq. (11) is called relative absorbance $ReAbs(\lambda)$.

The conversion to relative absorbance removes the partial information of chromophore such as melanin, oxy-hemoglobin, and deoxy-hemoglobin, which is unnecessary for the estimation. This is because the information removed by the conversion is the component immutable against wavelengths, which includes shading information. The component cannot be decomposed into chromophore information and shading information. Thus, the component is not necessary for the estimation:

$$Fnc(Abs(\lambda)) = \frac{1}{N} \times \sum_{\lambda} Abs(\lambda). \tag{11}$$

2.5 The method to estimate components concentration in skin tissue

This section describes the proposed method to estimate melanin concentration, blood concentration, and oxygen saturation in skin tissue using the dataset constructed in Sect. 2.3.

First, spectral reflectance $Ref(\lambda)$ of skin, the internal reflectance $Ref_{diffuse}(\lambda)$, and the surface reflectance $Ref_{specular}(\lambda)$ have a relation of Eq. (12) [7, 8]:

$$Ref(\lambda) = Ref_{diffuse}(\lambda) + Ref_{specular}(\lambda). \tag{12}$$

In this method, specular reflectance reflected by skin surface is supposed to be removed by the method of Ojima et al. [18], because this method considers diffuse reflectance of skin tissue. Thus, $Ref(\lambda) = Ref_{diffuse}(\lambda)$ based on Eq. (12). The conversion shown in Eq. (13) is applied to the spectral reflectance data of the dataset to convert it into absorbance data:

$$Abs(\lambda) = -\log(Ref(\lambda)). \tag{13}$$

Second, the absorbance data are converted to the relative absorbance data according to the method to remove an influence of shading described in Sect. 2.4.

Third, based on the constructed dataset of relative absorbance data and corresponding combinations of components concentration in skin tissue, we create a function that inputs melanin concentration, blood concentration and oxygen saturation, and outputs the corresponding relative absorbance. This function is called the relative absorbance function $RA()$. The function is created by performing polynomial regression including higher order in which explanation variable is components concentration in skin tissue and target variable is relative absorbance. For the four-layered skin model, the relative absorbance function is based on the polynomial model shown in Eq. (14), and the loss function is shown in Eq. (15). In the five-layered skin model, the relative absorbance function is based on the polynomial model shown in Eq. (16), and the loss function is shown in Eq. (17):

$$RA([Mel], [Bld], [Oxy], \lambda) = \sum_{i=0}^{order} \sum_{j=0}^{order} \sum_{k=0}^{order} a_n \times [Mel]^i \times [Bld]^j \times [Oxy]^k, \tag{14}$$

$$RSS_{func} = \sum_{i=1}^{2527} [ReAbs(\lambda, i) - RA([Mel], [Bld], [Oxy], \lambda)]^2, \tag{15}$$

$$RA\left(\begin{matrix} [Mel], [Bld_{pap}], [Oxy_{pap}], \\ [Bld_{ret}], [Oxy_{ret}], \lambda \end{matrix}\right) = \sum_{i=0}^{order} \sum_{j=0}^{order} \sum_{k=0}^{order} \sum_{l=0}^{order} \sum_{m=0}^{order} a_n \times [Mel]^i \times [Bld_{pap}]^j \times [Oxy_{pap}]^k \times [Bld_{ret}]^l \times [Oxy_{ret}]^m, \tag{16}$$

$$RSS_{func} = \sum_{i=1}^{25,000} \left[ReAbs(\lambda, i) - RA\left(\begin{matrix} [Mel], [Bld_{pap}], [Oxy_{pap}], \\ [Bld_{ret}], [Oxy_{ret}], \lambda \end{matrix}\right) \right]^2, \tag{17}$$

where order is the order of the polynomial model, n is the number of terms in the polynomial model, [Mel] is melanin concentration in epidermis, [Bld] is blood concentration in dermis, and [Oxy] is oxygen saturation in dermis in 4-layered skin model. [Bld_{pap}] indicates blood concentration in papillary layer, [Oxy_{pap}] indicates oxygen saturation in papillary layer, [Bld_{ret}] indicates blood concentration of reticular layer, and [Oxy_{ret}] indicates oxygen saturation of reticular layer in 5-layered skin model. The order of the polynomial model order is a hyperparameter in this method. The optimization of the order of the polynomial model is discussed in chapter. 3.

Forth, we describe the method to estimate melanin concentration, blood concentration and oxygen saturation in skin tissue based on the constructed relative absorbance function $RA(\lambda)$. In the four-layered skin model, based on a loss function Eq. (18), the least-squares method is conducted to estimate melanin concentration in the epidermis layer [Mel], blood concentration [Bld] and oxygen saturation [Oxy] in the dermis layer. Here, as the wavelengths, 560, 570, 590 and 610 [nm] are adopted according to the report of Akaho et al. [7]. In the five-layered skin model, based on a loss function Eq. (19), the least-squares method is conducted to estimate melanin concentration in epidermis layer [Mel], blood concentration [Bld_{pap}] and oxygen saturation [Oxy_{pap}] in papillary layer, and blood concentration [Bld_{ret}] and oxygen saturation [Oxy_{ret}] in reticular layer. Here, as the wavelengths, 31 wavelengths sampled at intervals of 10 [nm] between a range of 400 [nm] to 700 [nm] are adopted, according to the report of Iuchi et al. [9]:

$$RSS_{est} = \sum_{\lambda} (ReAbs(\lambda) - RA([Mel], [Bld], [Oxy], \lambda))^2, \tag{18}$$

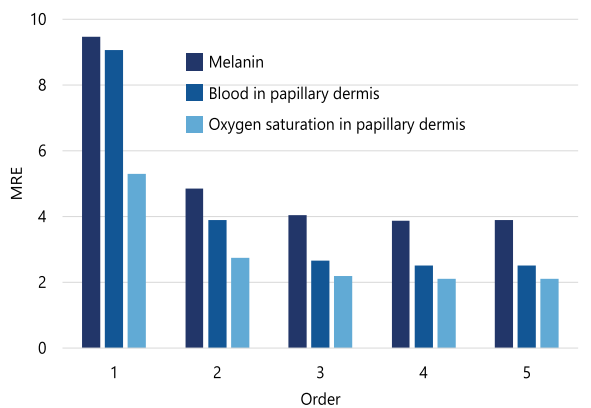
$$RSS_{est} = \sum_{\lambda} \left(ReAbs(\lambda) - RA \left(\begin{matrix} [Mel], [Bld_{pap}], [Oxy_{pap}], \\ [Bld_{ret}], [Oxy_{ret}], \lambda \end{matrix} \right) \right)^2. \tag{19}$$

3 Optimization of relative absorbance function

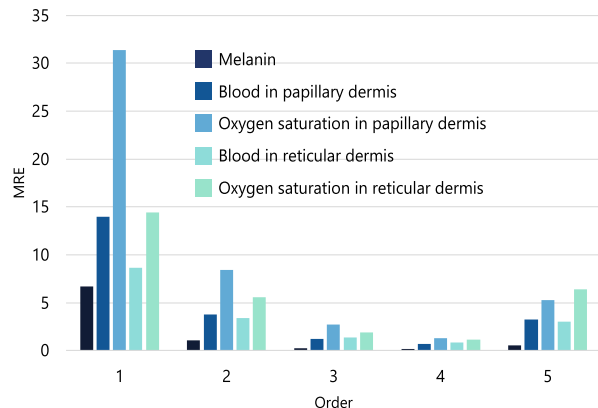
In this chapter, we compare the estimation accuracy of relative absorbance functions of different orders to select the best order for creating relative absorbance functions.

To select the most appropriate order for creating the relative absorbance function, we create relative absorbance functions of different orders and compare the estimation accuracy of these functions. The estimation accuracy is calculated using tenfold cross-validation. As an evaluation index we adapt mean relative error (MRE) [%], which is average of relative errors calculated by cross-validation. Relative error is defined by Eq. (21). Here, RelativeError denotes relative error, GroundTruth denotes ground truth, and EstimatedValue denotes estimated value based on the method.

Figure 7 shows the results of comparing each order of polynomial model for the four-layered skin model and five-layered skin models. Figure 7a shows the comparison of the estimation accuracy of the relative absorbance function based on different orders for the four-layered skin model, showing that fourth or fifth order has the lowest relative error for all components. Therefore, fourth order is considered to be the best for the four-layer skin model considering computational cost. Figure 7b shows the comparison of the estimation accuracy of the relative absorbance function based on different orders for the five-layered skin model,



(a) Based on four-layered skin model dataset



(b) Based on five-layered skin model dataset

Fig. 7 Results of comparing each order of polynomial model

showing that fourth order has the lowest relative error for all components. Therefore, fourth order is considered to be the best for the five-layer skin model.

4 Accuracy evaluation

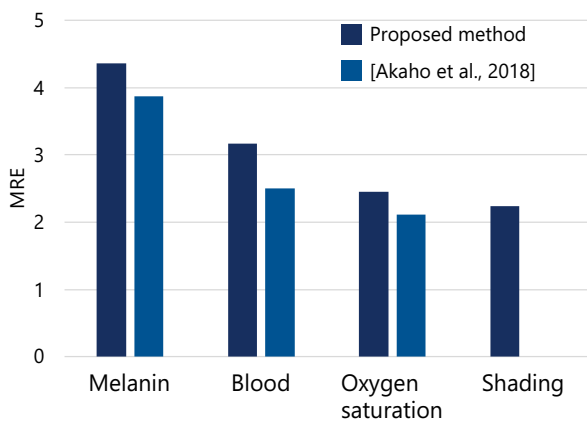
In this chapter, we compare the estimation accuracy between the proposed method and the previous methods proposed by Akaho et al. and Iuchi et al. [7, 8]. Here, the amount of data in dataset and the underlying skin model are different between our method and the previous method. In addition, in the method proposed by Iuchi et al., it is impossible to estimate oxygen saturation, and there are some immature points about the dataset, such as the fact that blood is not added to the layer where blood actually exists 8. Therefore, in this verification, the dataset is fixed to that of our method.

The accuracy verification is performed by tenfold cross-validation. To consider the influence of shading, shading is randomly added to the test data by Eq. (20) [7]. Here, $Ref(\lambda)$ indicates the spectral reflectance, $Ref_{sha}(\lambda)$ indicates the spectral reflectance after added shading, and k indicates the shading. The shading k has a random value in the range from 0 to 1 [7].

As an evaluation index we adapt Mean Relative Error (MRE), which is average of relative errors calculated by cross-validation. Relative error is defined by Eq. (21):

$$Ref_{sha}(\lambda) = Ref(\lambda) \times \exp(-k), \tag{20}$$

$$RelativeError = \left| \frac{GroundTruth - EstimatedValue}{GroundTruth} \right|. \tag{21}$$



(a) Based on four-layered skin model dataset

Figure 8a shows the evaluation result of the estimation accuracy of the four-layer skin model. This shows that the proposed method has improved accuracy compared to the previous method. Figure 8b shows the verification result of the estimation accuracy of the five-layer skin model. This indicates that the proposed method has improved accuracy compared to the previous method.

Comparing Fig. 8a, b, the estimation accuracy is relatively high in the five-layer skin model and the estimation accuracy is relatively small in the four-layer skin model. This result could be due to the difference of the number of the wavelengths used for the estimation. As we have described in Chapter 2, the number of the wavelength is four

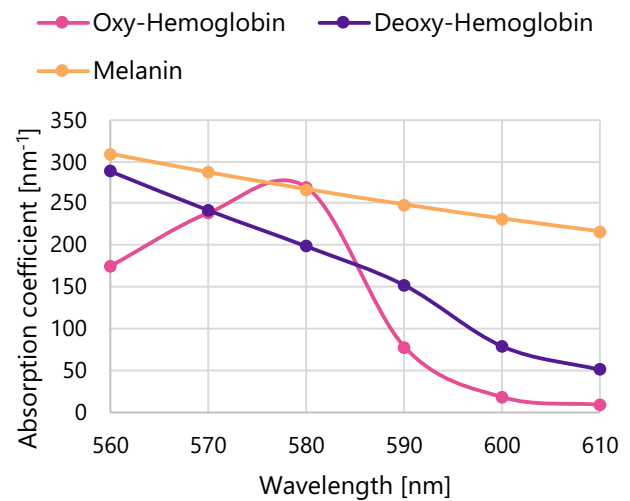
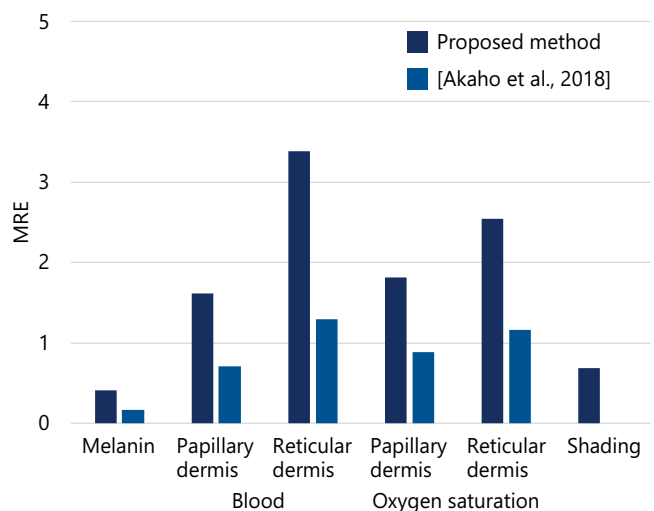


Fig. 9 Absorption coefficient of oxy-hemoglobin, deoxy-hemoglobin, and melanin of the wavelengths used for four-layered skin model



(b) Based on five-layered skin model dataset

Fig. 8 Accuracy verification results

for the four-layered skin model or 31 for the five-layered skin model. The greater number of the wavelengths means the greater number of the explanatory variables for the creation of the relative absorbance function based on the multiple regression. The greater number of the explanatory variables for multiple regression means the more accurate description of the relationship between the explanatory variable and the objective variable.

Besides, the comparison of Fig. 8a, b shows that the five-layered skin model is the higher improvement rate of the estimation accuracy than the four-layered skin model compared with the conventional method. This result could be caused by that in five-layered skin model shading error much more have influence on estimation of components concentration than in four-layered skin model since the five-layered skin model requires to detect small differences in absorbance compared to the four-layered skin model. This consideration is supported by the fact that there is a report that the main part of detected skin reflectance becomes localized in the topical skin layers including papillary dermis and upper blood net dermis [10].

In the four-layered skin model, the estimation accuracy of the melanin concentration is lowest in the components. This is considered to be due to the small difference among the absorbances of the used wavelengths. As shown in Fig. 9, the absorption coefficient of melanin has smaller variation depending on the wavelength than the one of oxy-hemoglobin or deoxy-hemoglobin within the range of the wavelengths used for four-layered skin model. This fact means that smaller feature of melanin is provided to the estimation based on the relative absorbance function than the one of oxy-hemoglobin or deoxy-hemoglobin.

The difference of the magnitude relationship of the estimation accuracy between the skin models is considered to be due to the similarity of the absorbance of the papillary dermis and reticular dermis. In the four-layered skin model, the components to be estimated have different the absorption coefficient as shown in Figs. 3 and 5. On the other hand, in the five-layered skin model, the part of the components to be estimated have the same absorption coefficient: the blood concentration or oxygen saturation in papillary dermis and in reticular dermis. This fact makes the estimation of the blood concentration and oxygen saturation in the five-layered skin model more difficult than the four-layered skin model.

5 Conclusion and future work

In this research, we have proposed the method to estimate melanin concentration, blood concentration and oxygen saturation in skin tissue with independence of shading considering depth-dependency of blood concentration. We have

constructed two types of skin model based on seven-layered skin model due to the tradeoff between the simplicity of skin model and the resolution of skin model. In addition, we have optimized the order of polynomial model. Finally, we have compared the estimation accuracy with the method proposed by Akaho et al. or by Iuchi et al., which have the highest accuracy of the methods to estimate components concentration in skin tissue based on two types of optical skin model. As a result, it has been shown that the proposed method had better capability of accurate estimation than the previous methods. As a future work, we chiefly have three tasks. First, we need verify applicability of the proposed method to actual measurement. In this research, we have verified the proposed method in simulation, but we have not verified the proposed in actual measurement. The final goal of this research is to apply this method to medical and beauty applications. Second, we need verify robustness of the proposed method to differences between constructed skin model and actual skin. In actual measurement, there is various differences between constructed skin model and actual skin such as thickness of skin tissue. Third, we need verify applicability of the proposed method to continuous measurement. The components concentration has temporal variation, which have rich information such as heart rate.

References

1. Dwyer PJ, Anderson RR, DiMarzio CA (1997) Mapping blood oxygen saturation using a multispectral imaging system. *Biomed Sens Imaging Track Technol II Int Soc Opt Photon* 2976:270–280
2. Tsumura N, Ojima N, Sato K, Shiraiishi M, Shimizu H, Nabeshima H, Akazaki S, Hori K, Miyake Y (2003) Image-based skin color and texture analysis/synthesis by extracting hemoglobin and melanin information in the skin. *ACM Transac Graph* 22(3):770–779
3. Kikuchi K, Masuda Y, Hirao T (2013) Imaging of hemoglobin oxygen saturation ratio in the face by spectral camera and its application to evaluate dark circles. *Skin Res Technol* 19:499–507
4. Shimada M, Masuda Y, Yamada MY, Itoh M, Takahashi M, Yatagai T (2000) Explanation of human skin color by multiple linear regression analysis based on the modified Lambert–Beer law. *Opt Rev* 7(4):348–352
5. Nishidate I, Maeda T, Niizeki K, Aizu Y (2013) Estimation of melanin and hemoglobin using spectral reflectance images reconstructed from a digital RGB image by the Wiener estimation method. *Sensors* 13:7902–7951
6. Kobayashi M, Ito Y, Sakauchi N, Oda I, Konishi I, Tsunazawa Y (2001) Analysis of nonlinear relation for skin hemoglobin imaging. *Opt Soc Am* 9(13):802–812
7. Akaho R, Hirose M, Tsumura N (2018) Evaluation of the robustness of estimating five components from a skin spectral image. *Opt Rev* 25(2):181–189
8. Iuchi K, Akaho R, Igarashi T, Ojima N, Tsumura N (2019) Estimation of blood concentrations in skin layers with different depths. In: 27th color and imaging conference, society for imaging science and technology, vol 1, pp 290–294
9. Wang L, Jacques S, Zheng L (1995) MCML—Monte Carlo modeling of light transport in multi-layered tissues. *Comput Methods Progr Biomed* 70(2):179–186

10. Meglinski IV, Matcher SJ (2003) Computer simulation of the skin reflectance spectra. *Comput Methods Progr Biomed* 70(2):179–186
11. Meglinski IV, Matcher SJ (2002) Quantitative assessment of skin layers absorption and skin reflectance spectra simulation in the visible and near-infrared spectral regions. *Physiol Meas* 23:741–753
12. Gemert MJC, Jacques SL, Sterenborg HJCM, Star WM (1989) Skin optics. *IEEE Trans Biomed Eng* 36(12):1146–1154
13. Svaasand LO, Norvang LT, Fiskerstrand EJ, Stopps EKS, Berns MW, Nelson JS (1995) Tissue parameters determining the visual appearance of normal skin and port-wine stains. *Lasers Med Sci* 10:55–65
14. Donner C, Jensen HW (2006) A spectral BSSRDF for shading human skin. In: *Eurographics symposium on rendering*, pp 409–417
15. Tsumura N, Kawabuchi M, Haneishi H, Miyake Y (2001) Mapping pigmentation in human skin from a multi-channel visible spectrum image by inverse optical scattering technique. *J Imaging Sci Technol* 45(5):444–450
16. Flynn CO, McCormack BAO (2009) A three-layer model of skin and its application in simulation wrinkling. *Comput Methods Biomech Biomed Eng* 12(2):125–134
17. Zhang R, Verkruysse W, Choi B, Viator JA, Jung B, Svaasand LO, Aquilar G, Nelson JS (2005) Determination of human skin optical properties from spectrophotometric measurements based on optimization by genetic algorithms. *J Biomed Opt* 10(2):024030
18. Ojima N, Minami T, Kawai M (1997), Transmittance measurement of cosmetic layer applied on skin by using processing. In: *Proceeding of the 3rd scientific conference of the Asia Societies of Cosmetic Scientists*, vol 114

Publisher's Note Springer Nature remains neutral with regard to jurisdictional claims in published maps and institutional affiliations.